



Dendritic growth velocity and diffusive speed in solidification of undercooled dilute Ni-Zr melts

M. Schwarz^a, C.B. Arnold^b, M.J. Aziz^b, D.M. Herlach^a

^a Institut für Raumsimulation, DLR, D-51140 Köln, Germany

^b Division of Engineering and Applied Sciences, Harvard University, Cambridge, MA 02138, USA

Abstract

During rapid solidification of undercooled melts deviations from local equilibrium occur at the solid-liquid interface. With increasing interface velocity v , the interfacial undercooling ΔT_i increases and solute trapping becomes important. These phenomena are well characterized for planar interfaces, but for dendritic growth they must be incorporated into dendrite growth theory and the combination tested. The predictions of dendrite growth theory are very sensitive to the diffusive speed—the interface speed at which the solute trapping function is in mid transition between local equilibrium and complete trapping. Dendrite growth velocities have been measured as a function of undercooling in levitated droplets of Ni₉₉Zr₁ alloys. The results are described within current theory of dendrite growth taking into account deviations from local equilibrium. The diffusive speed is independently determined by preliminary pulsed laser melting experiments on thin film specimens for the same alloy system. Best fit values of the diffusive speed inferred from both sets of measurements are similar in magnitude. Given the preliminary nature of the pulsed laser melting measurements, this result is encouraging for the prospects of a parameter-free test of modern dendrite growth theory. © 1997 Elsevier Science S.A.

Keywords: Rapid solidification; Dendrite growth; Solute trapping

1. Introduction

Undercooling of a melt gives rise to a driving force for crystallization due to the difference between the Gibbs free energy of the undercooled liquid phase and that of the solid phase. For deeply undercooled melts, the driving force for resolidification becomes large enough to move the system into the regime of rapid solidification where assumptions of local equilibrium break down. This deviation from local equilibrium manifests itself as a local undercooling of the interface and as a deviation from the chemical equilibrium at the solid-liquid interface. Modern dendrite growth models [1,2] take into account such non-equilibrium effects by introducing a kinetic undercooling of the solid-liquid interface and a dependence of the partition coefficient on the growth velocity. The latter effect is described by the solute-trapping model of Aziz [3]. In the dilute concentration limit of alloys the velocity dependence of the partition coefficient $k = k(v)$ is expressed by:

$$k = \frac{k_e + v/v_D}{1 + v/v_D}, \quad (1)$$

where k_e is the equilibrium partition coefficient, v is the interface velocity and v_D , the diffusive speed, is treated as a free parameter. Laser resolidification experiments on thin films in combination with the determination of concentration profiles in the as-solidified samples by Rutherford backscattering spectroscopy (RBS) enable the measurement of $k(v)$ and therefore a determination of v_D as well. Such experiments on a variety of different dilute alloys have confirmed the validity of Eq. (1) for planar growth in thin films [4-7].

In the case of undercooled melts we have to deal with free dendritic growth. At large undercoolings, the driving force can cause dendrite growth velocities in the range of 1-100 m s⁻¹ [8,9] which are comparable with rapid crystal growth in laser resolidification experiments. The analysis of dendrite growth theory assumes the validity of Eq. (1) even though there is not a planar interface. In the present work both the dendrite growth velocity is measured as a function of undercooling and the diffusive speed in laser heat melted thin films on the same sample system of dilute Ni-Zr alloys. The combination of these results may be used to describe rapid dendrite growth without any adjustable parameter.

2. Experimental details

Electromagnetic levitation is used for containerless undercooling of bulk drops [10]. The experiments are conducted in a UHV chamber which was evacuated to a pressure of 10^{-7} mbar and backfilled with a purified He-H₂ gas mixture (20 vol.% H₂). The avoidance of container-wall induced nucleation and highly pure environmental conditions leads to reproducible maximum undercoolings of $\Delta T = 300$ K prior to nucleation. The freely suspended drops are accessible to direct observations of rapid solidification and the temperature of the sample is measured at its top by a two-color pyrometer with an accuracy of ± 5 K. Crystallization of the undercooled melt is stimulated at its lower end by using an Alumina stimuli needle. The solidification starts at this well defined point and the array of dendrites grows radially into the melt. A rapid photosensing technique is utilized to measure the velocity of the advancing solidification front as a function of undercooling [11]. The pyrometrically detected temperatures of a small square area of the sample surface were read into a transient recorder at a sampling rate of up to 1 MHz. The time, Δt , needed by the envelope of the dendrite tips to sweep across the sensitive area of the photodiode of the width Δs is measured, and the dendrite growth velocity is given by $v = \Delta s / \Delta t$. The results of these velocity-undercooling measurements are analyzed within current dendrite growth models [1,2].

The diffusive speed is independently measured by a pulsed-laser resolidification technique described elsewhere [4–7]. A thin film (~ 2700 Å) of Ni was deposited by electron beam evaporation on an Si wafer covered with 2000 Å of thermally grown SiO₂. Ion implantation of ⁹⁰Zr⁺ was used to place the peak in solute concentration at 300 Å beneath the free surface. The wafers were then patterned and etched for transient reflectance and transient conductance measurements of interface positions and velocities. Laser melting was performed with a single 35 ns excimer laser pulse (KrF: 248 nm) at fluences of 0.4–0.7 J cm⁻² to yield a solidification velocity of 2.8 m s⁻¹. Initial and final concentration profiles of Zr were obtained using RBS grazing-angle techniques [7] which produce a depth resolution of 60 Å. The analysis of the diffusive speed was performed by comparing the measured final concentration profile to one predicted by computer simulation. The simulation utilized a Crank–Nicholson algorithm to solve the 1-dimensional diffusion equation for the molten portion of the sample. The values of the liquid diffusivity and the diffusive speed are then determined by a best fit between the experimental and simulated curves.

Dilute Ni₉₉Zr₁ alloys were chosen for the present experiments because of several considerations. They are undercoolable by electromagnetic levitation experi-

ments. Another favorable property of the Ni-Zr system at small Zr amounts is its small equilibrium partition coefficient k_e on the order of 10^{-3} . Therefore, a strong solute trapping effect is expected at growth velocities which are observable both in the undercooling experiment as well as in the laser resolidification experiments. An additional requirement for the measurements of the partition coefficient by RBS is that the solute (Zr) be significantly heavier than the solvent in order to resolve the solute depth profile. For the electromagnetic levitation experiment, alloys of Ni₉₉Zr₁ were prepared from constituents of Ni and Zr both of a purity better than 99.99%. They were melted in situ under a high purity He gas atmosphere in a radio frequency levitation coil into spheres of about 6 mm diameter. The mass of the sample amounts to about 1 g. For the laser resolidification experiment, the Ni used for evaporation was 99.99% and the Zr was implanted to give a peak concentration of 0.5–1 atomic percent.

3. Experimental results and discussion

3.1. Measurement of dendrite growth velocities

Fig. 1 shows the experimental results for the measurements of the dendrite growth velocity as a function of undercooling on dilute Ni₉₉Zr₁ alloy (cf. dots in Fig. 1). At small undercooling the growth velocity is rather sluggish. If the undercooling approaches a critical undercooling of $\Delta T_{CR} \approx 190$ K a steep rise of the growth velocity with increasing undercooling is observed. Such a behaviour in the velocity versus undercooling relation has previously found in dilute Ni-B alloys [9].

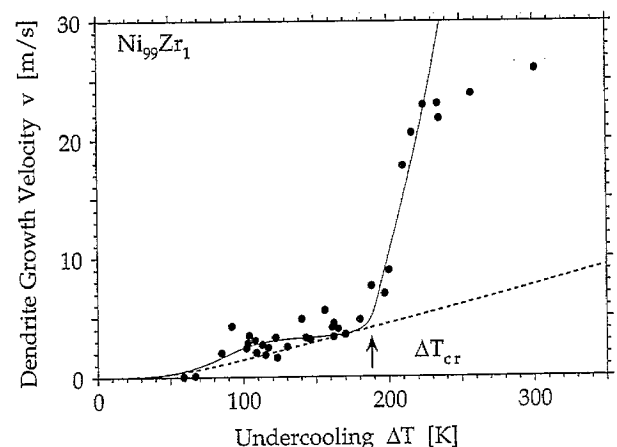


Fig. 1. Dendrite growth velocity v as a function of undercooling ΔT for Ni₉₉Zr₁. Experimental results are represented by the dots. The solid line gives the prediction of dendrite growth theory taking into account a velocity dependent partition coefficient. For comparison, the dotted line gives the results of computations within dendrite growth theory but neglecting solute trapping. A satisfactory description of the experimental results can only be achieved if a velocity dependent partition coefficient is taken into consideration.

Table 1
Material parameters used for the calculation of the dendrite growth velocities as a function of undercooling

Heat of fusion	ΔH [J mol ⁻¹]	17150
Specific heat of the liquid	c_p^l [J mol ⁻¹ K ⁻¹]	41
Thermal diffusivity	D_T [m ² s ⁻¹]	9 e-6
Diffusion coefficient	D_L [m ² s ⁻¹]	2 e-9
Equilibrium partition coefficient	k_e	2.8 e-3
Diffusive speed	v_D [m s ⁻¹]	20
Liquidus slope	m [K at.%]	-14.1
Speed of sound	v_0 [m s ⁻¹]	4000

For an analysis of the experimental results we apply current theories of dendrite growth [1,2]. Correspondingly, the total undercooling ΔT is expressed as the sum of four different terms:

$$\Delta T = \Delta T_t + \Delta T_c + \Delta T_r + \Delta T_k, \quad (2)$$

with the individual contributions of the thermal undercooling ΔT_t , the constitutional undercooling ΔT_c , the curvature undercooling ΔT_r and the kinetic (interface friction) undercooling ΔT_k . These are expressed as

$$\Delta T_t = \frac{\Delta H_f}{c_p^l} F_{IV}(P_t) \quad (2a)$$

$$\Delta T_c = mc_0 \left(1 - \frac{m^*/m}{1 - (1 - k(v))F_{IV}(P_c)} \right) \quad (2b)$$

$$\Delta T_r = \frac{2\Gamma}{R} \quad (2c)$$

$$\Delta T_k = \frac{v}{\mu} \quad (2d)$$

Here, $F_{IV}(x) \equiv x \exp(x)E_1(x)$ denotes the Ivantsov function (with E_1 the first exponential integral function), $P_t = vR/2D_T$ the thermal Péclet number (with v the interface velocity, R the curvature radius of the dendrite tip), m^* the velocity dependent liquidus slope, c_0 the nominal concentration of the alloy, $P_c = vR/2D_L$ the chemical Péclet number, $G = s/DS_f$ the Gibbs-Thomson coefficient (with s the solid-liquid interface energy, ΔS_f the entropy of fusion), $\mu = (\Delta H_f v_0)/(k_B T_L^2)$ the interfacial kinetic coefficient according to the model of collision limited growth [12] (with k_B the Boltzmann constant) and T_L the liquidus temperature. The other symbols are explained in Table 1.

Eq. (2) describes the undercooling in terms of the product of the growth velocity v times the dendrite tip radius R . For a unique calculation of the dendrite growth velocity as a function of undercooling we use the criterion of marginal stability [13] which gives an expression of the dendrite tip radius:

$$R = 4\pi^2 \Gamma \left[\frac{\Delta H_f}{c_p^l} P_t \xi_t - \frac{2 \cdot m \cdot c_0 (1 - k(v)) P_c}{1 - (1 - k(v)) F_{IV}(P_c)} \xi_c \right]^{-1} \quad (3)$$

where

$$\xi_t = 1 - (1 + (2\pi/P_t)^2)^{-1/2} \quad (3a)$$

and

$$\xi_c = 1 - \frac{2k}{2k - 1 + (1 + (2\pi/P_c)^2)^{1/2}} \quad (3b)$$

The solid line in Fig. 1 represents the results of the calculations according to Eq. (2) and Eq. (3) if the material parameters are used for the computations as listed in Table 1. In the undercooling range of $\Delta T \leq 220$ K the measured data are well described by theory. In particular, the steep rise of the growth velocity in the vicinity of the critical undercooling ΔT_{cr} is predicted by theory in a correct way. For comparison, the dotted line in Fig. 1 shows the equivalent result of the growth velocity calculation with the solute trapping effect neglected. The measured data can only be reproduced by the theory if a velocity dependent partition coefficient is used to calculate the constitutional undercooling ΔT_c . Hence, solute trapping has a pronounced influence on the $v - \Delta T$ relation.

For a further analysis of solute trapping during rapid dendrite growth the concentrations at the dendrite tip in the liquid c_L is calculated according to

$$c_L = \frac{c_0}{1 - (1 - k(v)) \cdot F_{IV}(P_c)} \quad (4)$$

The concentration in the solid c_s is then found by applying the definition of the partition coefficient, $c_s = k \cdot c_L$. The results of these computations are plotted as a function of the undercooling in Fig. 2. At small undercoolings the Zr concentration in the liquid rises due to the rejection of the solute atoms (limited solubility) and

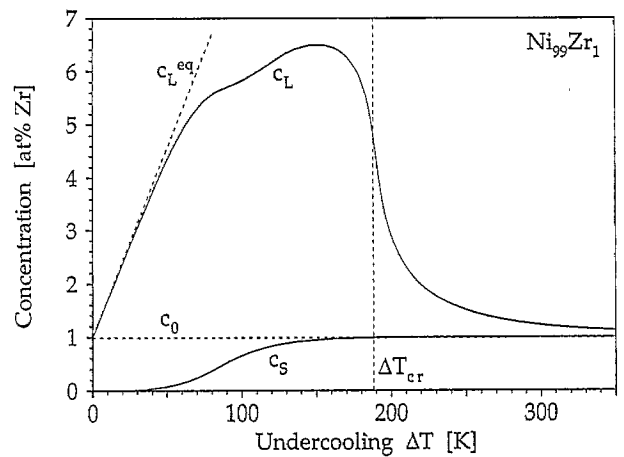


Fig. 2. Concentration profiles in the liquid, c_L , and in the solid state, c_s , at the interface. At small undercoolings partitioning occurs under equilibrium conditions while with increasing undercooling deviations occur from the equilibrium because of solute trapping. This finally leads to complete partitionless solidification in the range $\Delta T > \Delta T_{cr}$, indicated by the fact that both the c_L and c_s profiles approach the nominal concentration c_0 .

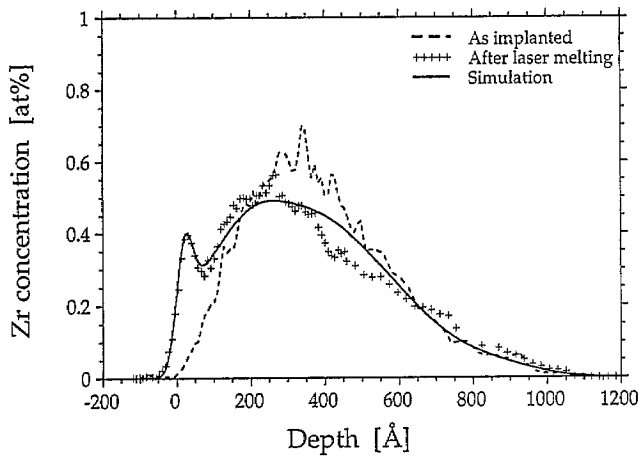


Fig. 3. Zr composition versus depth for a 2700 Å film which solidified at 2.8 m s^{-1} . The sample was irradiated with a 0.52 J cm^{-2} 35-ns pulse. The simulation was performed with $v_D = 28 \text{ m s}^{-1}$ and a liquid diffusivity $D_L = 0.65 \times 10^{-9} \text{ m}^2 \text{ s}^{-1}$. We notice a close fit of the data in the near surface region ($< 250 \text{ Å}$) of the sample however, the fit in the deeper region (250–700 Å) appears less accurate. The differences in this latter region suggests potential pathologies in our resolidification process that require further investigation.

the concentration profiles follow the equilibrium values (cf. solid lines in Fig. 2). This means there is strong partitioning in front of the slowly advancing interface. If the undercooling is increased into the regime $\Delta T > 90 \text{ K}$ deviations occur which progressively rise with undercooling. At large undercoolings $\Delta T > \Delta T_{cr} = 190 \text{ K}$ c_L approaches the nominal concentration c_0 of the alloy. This means at such undercoolings we have reached a regime of complete solute trapping.

With these results in mind the behaviour of the velocity–undercooling relation is understood. At small undercoolings the interface movement is sluggish and controlled by the redistribution of solute in front of the interface. If solute trapping becomes important, the concentration gradient becomes weaker until it diminishes at undercoolings in the vicinity or above ΔT_{cr} . In this undercooling range the constitutional undercooling loses its influence and the growth velocity is only controlled by the thermal gradient in front of the solid–liquid interface. The chemical diffusion coefficient is smaller by three orders of magnitude than the thermal diffusivity. As a consequence, the growth velocity steeply rises in the transition regime around ΔT_{cr} .

3.2. Preliminary measurement of the diffusive speed

Fig. 3 shows the comparison of the simulated Zr concentration profile to the experimentally measured solute concentration profile. For this simulation, the maximum melt depth was 1800 Å and the resolidification velocity was 2.8 m s^{-1} . The initial concentration profile is allowed to evolve while in the liquid phase according to the diffusion equation using a liquid diffu-

sivity of $0.65 \times 10^{-9} \text{ m}^2 \text{ s}^{-1}$. This causes a depression of the main peak in the profile as Zr moves to regions of lower concentration. As the sample resolidifies, the interface moves toward the surface causing rejected Zr to pile up in front of the moving interface; eventually the interface reaches the free surface of the film where it deposits the accumulated Zr. This effect creates by the characteristic peak in the concentration profile at the surface in both the simulated and the experimental curves.

The numerical values of $v_D = 28 \text{ m s}^{-1}$ and $D_L = 0.65 \times 10^{-9} \text{ m}^2 \text{ s}^{-1}$ obtained by the laser resolidification method are comparable to $v_D = 20 \text{ m s}^{-1}$ and $D_L = 2.0 \times 10^{-9} \text{ m}^2 \text{ s}^{-1}$ as used for the calculation of the dendrite growth velocity in the undercooling experiment. It should be noted that the results from laser resolidification are still in a preliminary stage. The differences between the simulated concentration profile and the final concentration profile in the region 250–750 Å suggest that our results could be prone to certain experimental pathologies. For example, there exists the possibility for interfacial breakdown during resolidification as well as surface gettering of the segregated Zr. Surface gettering would place an artificial high amount of Zr in the surface peak and therefore cause an overestimate of v_D . Interfacial breakdown could also result in an artificially high amount of Zr left in deeper regions of the sample and would make our liquid diffusivity appear low. Further investigation must be done before a final result may be obtained. However, given the uncertainties in the laser results at present, the proximity of the combined results should be considered encouraging for the success of dendrite growth theory.

4. Conclusion

In the present work we have measured the dendrite growth velocities as a function of undercooling using electromagnetic levitation to obtain containerless undercooling on bulk $\text{Ni}_{99}\text{Zr}_1$ alloys. In addition, we have independently obtained the diffusive speed by laser resolidification experiments on thin films of the same alloy for a single growth velocity. The results from laser resolidification are still preliminary. However, they suggest that a fit of the dendrite growth theory without any adjustable parameters is possible.

Acknowledgements

The authors thank Dr K. Eckler for stimulating discussions. Financial support by the Deutsche Forschungsgemeinschaft within contract No. He 1601/4-1 is gratefully acknowledged. Work at Harvard University was supported by NSF-DMR-92-08931. In

addition, one of us (C.B.A.) acknowledges the support of an ONR graduate student fellowship.

References

- [1] J. Lipton, W. Kurz and R. Trivedi, *Acta Metall.*, 35 (1987) 957.
- [2] W.J. Boettinger, S.R. Coriell and R. Trivedi, in R. Mehrabian and P.A. Parrish (eds.), *Rapid Solidification Processing-Principles IV*, Claitor's, Baton Rouge, 1988, p. 13.
- [3] M.J. Aziz and T. Kaplan, *Acta Metall.*, 36 (1988) 2335.
- [4] M.J. Aziz, J.Y. Tsao, M.O. Thompson, P.S. Peercy and C.W. White, *Phys. Rev. Lett.*, 56 (1986) 2489.
- [5] D.E. Hoglund, M.J. Aziz, S.R. Stiffler, M.O. Thompson, J.Y. Tsao and P.S. Peercy, *J. Cryst. Growth*, 109 (1991) 107.
- [6] M.J. Aziz, *Mater. Met. Mat. Trans. A*, 27 (1996) 671.
- [7] P.M. Smith and M.J. Aziz, *Acta metall. mater.*, 42 (1994) 3515.
- [8] R. Willnecker, D.M. Herlach and B. Feuerbacher, *Phys. Rev. Lett.*, 62 (1989) 2709.
- [9] K. Eckler, R.F. Chochrane, D.M. Herlach and B. Feuerbacher, *Phys. Rev. B*, 45 (1992) 5019.
- [10] D.M. Herlach, R. Willnecker and F. Gillessen, in: *Proc. 5th Eur. Symp. Mater. Sci. under Microgravity*, ESA SP-222, Schloss Elmau, 1984, pp. 399.
- [11] E. Schleich, R. Willnecker, D.M. Herlach and G.P. Görler, *Mater. Sci. Eng.*, 98 (1988) 39.
- [12] D. Turnbull, *Metall. Trans. A*, 12 (1981) 693.
- [13] J.S. Langer and H. Müller-Krumbhaar, *Acta Metall.*, 26 (1978) 1689, 26 (1978) 1697.